

## Resonantly Enhanced Electron Tunneling Rates in Quantum Wells

G. Livescu,<sup>(a)</sup> A. M. Fox, D. A. B. Miller, T. Sizer, and W. H. Knox  
*AT&T Bell Laboratories, Holmdel, New Jersey 07733*

A. C. Gossard and J. H. English  
*Materials Department, University of California, Santa Barbara, California 93106*  
 (Received 17 February 1989)

Resonant tunneling of electrons in GaAs/AlGaAs quantum wells is resolved by picosecond pump-and-probe electroabsorption measurements. The temperature-independent tunneling escape times are dramatically affected by the applied electric field, with a pronounced minimum at the field corresponding to the resonance between the  $n=1$  electron level in one quantum well, and the  $n=2$  electron level in the adjacent one. The calculated field dependence of the tunneling times is in qualitative agreement with the data.

PACS numbers: 78.50.Ge, 72.20.Jv, 73.40.Gk, 78.20.Jq

The investigation of the tunneling of particles through potential barriers in semiconductor quantum wells has recently attracted much attention. Intense research has focused on basic quantum effects ranging from Bloch transport of electrons and holes in minibands<sup>1</sup> to resonant and nonresonant tunneling in samples with wider barriers,<sup>2</sup> in a variety of material systems such as GaAs/AlAs,<sup>3-6</sup> GaAs/AlGaAs,<sup>7-11</sup> and InGaAs/InP.<sup>2,12,13</sup> In spite of the large amount of work, there are still many open questions concerning dynamical aspects of the vertical transport. Our purpose here is to study the mechanisms by which carriers escape from quantum wells under the influence of an electric field. The results are also relevant for the speed limits of electro-optical devices using electroabsorption in semiconductor quantum wells.<sup>14</sup>

Most of the experimental effort in this field has concentrated on steady-state photocurrent<sup>2,4,5</sup> and optical<sup>4,7,13</sup> measurements, providing only very indirect information on the dynamics of the transport. Time-resolved techniques are required for the direct study of transport processes. For example, it is possible to inject a short charge pulse into one contact of the sample and to measure the transmitted current pulse at the other contact in real time.<sup>4,5</sup> Or, one can generate carriers directly in the quantum wells by absorption of photons from a short laser pulse. The photoinduced carrier population may then decay by recombination, thermionic emission, or tunneling through the barriers. One way of studying the loss of carriers is time-resolved photoluminescence spectroscopy, as shown in the pioneering work of Deveaud *et al.*<sup>1</sup> and Tsuchiya, Matsusue, Sasaki,<sup>3</sup> and more recently by Jackson *et al.*<sup>7</sup>

We have chosen a new approach, that of time-resolved electroabsorption measurements.<sup>10,11</sup> A picosecond laser pump pulse is used to excite carriers in quantum wells contained in the intrinsic region of a reverse-biased  $p-i-n$  structure. The carriers that escape from the quantum wells are swept by the field towards the electrodes. This separation of charge locally reduces the voltage between

the electrodes and alters the absorption coefficient via the quantum-confined Stark effect (QCSE).<sup>15</sup> The time dependence of the absorption change  $\Delta\alpha(t)$  is monitored with a time-delayed probe pulse, providing information about the escape rate of the carriers. The experiment has a pulse-width-limited resolution of  $\sim 10$  ps. By studying the effects of the applied field on the rise time  $\tau$  of  $\Delta\alpha$  at temperatures of 100 and 300 K, we are able to identify tunneling of electrons through the barriers as the dominant carrier escape mechanism. We find that the temperature-independent tunneling times vary between a few hundreds of ps at low fields and a few tens of ps at high fields, with a pronounced minimum at an intermediate field where the  $n=1$  electron level in one quantum well is in resonance with the  $n=2$  electron level in the adjacent one. Our results clearly demonstrate that this dependence is the signature of resonant tunneling.

The sample used was a  $p-i-n$  structure grown by molecular-beam epitaxy, containing 75 periods of 65-Å/57-Å GaAs/Al<sub>0.31</sub>Ga<sub>0.69</sub>As quantum wells in its intrinsic region. The thickness of the layers and the Al concentration were obtained from the growth parameters, and from optical and electron microscope measurements.<sup>16</sup> Using photolithographic techniques, contacts were made to the doped regions, with  $200 \times 200 \mu\text{m}^2$  windows on the  $p$  side. The samples were antireflection coated and the substrate was etched away. The transmission spectrum at room temperature [inset of Fig. 1(a)] shows the excitonic peaks associated with the allowed  $n=1$  and  $n=2$  transitions. By applying a voltage  $V$  the allowed peaks shift to longer wavelength and broaden. The field  $F$  inside the sample may be estimated from  $F = (V + V_{\text{bi}})/d$ , where  $V_{\text{bi}} = 1.5$  V is the built-in potential, and  $d = 0.9 \mu\text{m}$  is the thickness of the intrinsic region of the diode. The shifts of the  $n=1$  heavy-hole ( $E_{1\text{hh}}$ ) and light-hole ( $E_{1\text{lh}}$ ) excitonic peaks could be followed up to an applied voltage of 30 V (estimated field of  $3.5 \times 10^5$  V/cm) and were found to be in reasonable agreement with those predicted by the QCSE theory.<sup>15</sup>

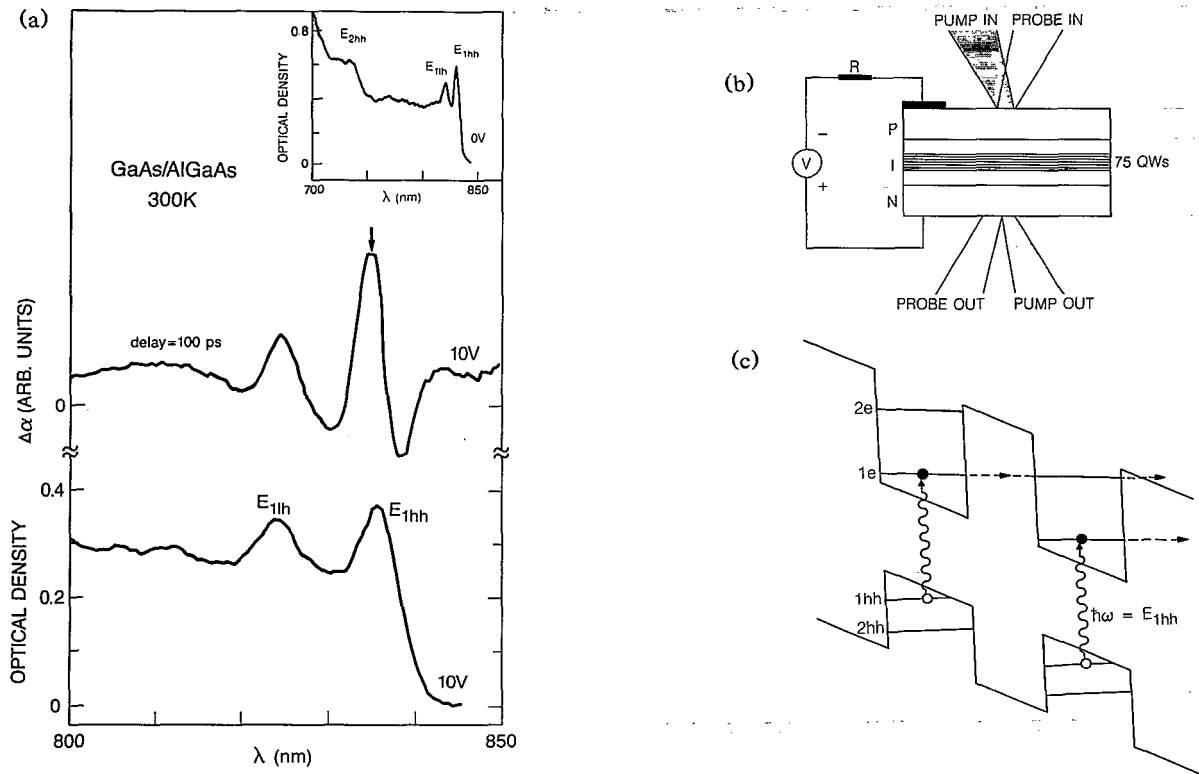


FIG. 1. (a) Room-temperature absorption spectra of the *p-i-n* modulator at 0 V (inset) and 10 V (lower curve). The upper curve is the room-temperature differential absorption spectrum at 10 V and 100 ps after excitation. Arrow: wavelength used for time-resolved measurements at 10 V. The estimated field at 10 V is  $1.2 \times 10^5$  V/cm. (b) Biasing circuit and geometry used in pump-and-probe experiment. (c) Schematic diagram of the electron (1e, 2e) and heavy-hole (1hh, 2hh) confined levels at resonance. The carriers are photogenerated in the 1e and 1hh states after the absorption of photons at energy  $\hbar\omega = E_{1lh}$ . The dotted arrow indicates tunneling of the electron from the 1e state in one well to the 2e state in the adjacent one.

For the time-resolved measurements we used a conventional pump-and-probe arrangement. Both beams were derived from the same synchronously pumped Styryl 9 dye laser (6–10-ps pulse width, 790–870-nm tuning range), and were focused to  $\sim 25$ - $\mu\text{m}$ -diam spots overlapping on the sample [Fig. 1(b)]. In order to minimize the space-charge effects of the carriers we used low optical powers: 20–50  $\mu\text{W}$  (0.24–0.6 pJ per pulse) for the exciting beam, and 5  $\mu\text{W}$  for the probe. The number of photoexcited carriers per pulse was  $(2-5) \times 10^{15} \text{ cm}^{-3}$ . The energy of the exciting beam was close to  $E_{1lh}$ , generating electrons and heavy holes with very small kinetic energy near the lowest allowed confined levels, 1e and 1hh [see Fig. 1(c)]. The carriers are generated in all the wells throughout the sample, although their concentration decreases somewhat as the exciting beam exits the quantum well region. We detected the changes in the intensity of the transmitted probe using standard lock-in techniques. An example of the data is shown in Fig. 1(a). Represented here is the spectrum of  $\Delta\alpha$  at a reverse bias of 10 V (estimated field of  $1.2 \times 10^5$  V/cm), probed 100 ps after the exciting pulse. This differential absorption spectrum indicates a blue shift and an increase in oscillator strength of both  $E_{1lh}$  and

$E_{1lh}$  excitons, consistent with a reduction  $\Delta V$  of the applied voltage. The time-resolved measurements were done in the vicinity of the  $E_{1lh}$  exciton, at the wavelength corresponding to the largest positive  $\Delta\alpha$  at each voltage, as shown by the arrow in Fig. 1(a). The magnitude of  $\Delta\alpha$  is affected by the power of the exciting beam:  $\Delta\alpha$  is roughly proportional to  $\Delta V$ , which is determined by the total number of photoexcited carriers. We were able to confirm the proportionality of  $\Delta\alpha$  with the pump power over more than 1 order of magnitude; importantly, this rules out any possible artifacts from an overall build-up of space charge in the sample. The time dependence of  $\Delta\alpha$  measured at different applied fields is illustrated in Fig. 2. Both the rise and decay times appear to be field dependent; large fields are associated with larger signals, having faster rise and fall times. While the rise time  $\tau$  of  $\Delta\alpha$  (thus  $\Delta V$ ) is determined by the vertical transport of the carriers, its decay is related to the mechanism of recovery of  $\Delta\alpha$ . In our previous work<sup>11</sup> we have shown that the recovery of  $\Delta V$  proceeds by a mechanism of diffusive electromagnetic propagation over the area of the *p* and *n* electrode layers:  $\Delta V(t) \sim (1+t/t_c)^{-1}$ . Note that this rapid electromagnetic propagation is not to be confused with the much slower actual diffusion of the

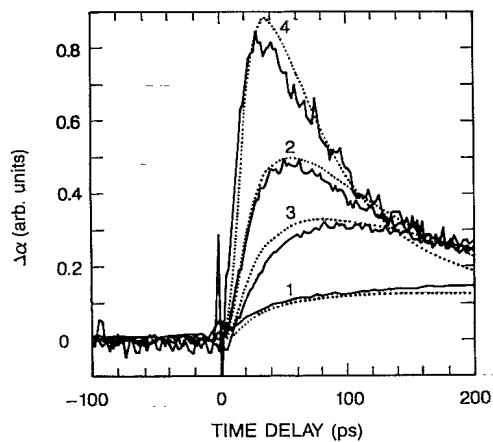


FIG. 2. Room-temperature differential absorption at different applied fields vs time delay after excitation. Full lines: experimental; dotted lines: calculated. The curves correspond to the following values of the applied field and rise time  $\tau$ : (curve 1)  $10^5$  V/cm, 375 ps; (2)  $1.2 \times 10^5$  V/cm, 60 ps; (3)  $1.6 \times 10^5$  V/cm, 120 ps; (4)  $2.4 \times 10^5$  V/cm, 25 ps.

photogenerated carriers. The diffusive time constant  $t_c = w^2 R_{sq} C_A$ , with  $w$  the exiting spot diameter,  $R_{sq}$  the resistance per square of the contact layers, and  $C_A$  the capacitance per unit area. For our sample and spot size,  $t_c \sim 5$  ps. The buildup of the voltage pulse  $\Delta V$  induced by the vertical movement of the carriers towards the contacts is thus competing with the lateral spread of  $\Delta V$  over the area of these conducting regions. As a result, the overall time dependence of  $\Delta\alpha$  will be given by the convolution of the rising exponential  $[1 - \exp(-t/\tau)]$  and the decaying function  $(1 + t/t_c)^{-1}$ . For  $\tau \gg t_c$ ,  $\Delta V$  will start decaying before the majority of the carriers arrive at the electrodes, resulting in a small and very slowly rising signal, whose decay essentially shows the slow end of the function  $(t + t/t_c)^{-1}$  (see curves 1 and 3 in Fig. 2). Hence our experiment is relatively insensitive to any slow emission process. For  $\tau \sim t_c$ ,  $\Delta V$  can be built up to a larger value before it starts decaying. The result in this case is a faster rising, larger signal, followed by a faster decay (see curves 2 and 4 in Fig. 2). While  $t_c$  is a constant for a given structure,  $\tau$  should depend on the applied field, and regardless of the particular escape mechanism of the carriers, it should become shorter at larger fields. This is indeed what our data show (Fig. 2). The dotted curves are calculated with our complete diffusive conduction model,<sup>11</sup> with  $\tau$  the only fitting parameter.

Our main emphasis here is the measurement of the rise times  $\tau$  and their dependence on the applied field. In Fig. 3(a) we show the experimental data obtained at room temperature (open circles) and at 100 K (filled circles). Two key results are evident: The rise times are (1) practically independent of temperature, and (2) strongly affected by the applied field. A sharp decrease of  $\tau$  with increasing field is observed, with a clear

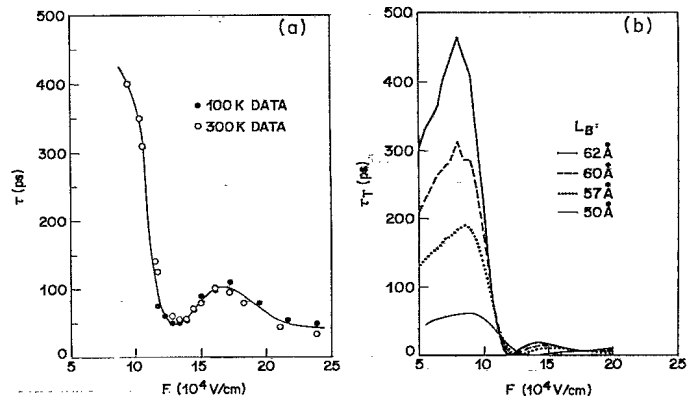


FIG. 3. (a) Differential absorption rise time vs applied field. Open circles: data at 300 K; filled circles: data at 100 K. The line connecting the data points is a guide for the eyes. (b) Calculated electron tunneling times  $\tau_T$  vs electrical field, for the structure of Fig. 1(c). The parameters used are listed in the text; the barrier widths  $L_B$  corresponding to the different curves are indicated.

minimum around  $1.2 \times 10^5$  V/cm. Since  $\tau$  is independent of temperature, it is more likely that the carrier escape mechanism seen here is tunneling, as previously reported in GaAs/AlAs double-barrier structures.<sup>3,7</sup> Furthermore, the presence of a minimum in  $\tau$  strongly suggests that resonant tunneling occurs; importantly, we find that the position of this minimum agrees with the field which we have calculated for alignment of the first electron level ( $1e$ ) in one well with the second electron level ( $2e$ ) in the adjacent one. Hence we believe we see in these data resonant tunneling of the electrons between adjacent wells.

We do not see any features that we can ascribe to resonant tunneling of holes. This is not unexpected, since heavy-hole tunneling probabilities are typically  $\sim 500$  times smaller than those of electrons. On the other hand, we do not see any evidence of space-charge effects from hole buildup. This means that the holes eventually escape too, in times shorter than the interval between consecutive laser pulses (12 ns). Note that  $\Delta\alpha$  is a measure of the local voltage change  $\Delta V$  on the electrodes, which in turn is induced by the dipole created by the increasing separation between the drifting electrons and the holes (whether the latter are also drifting or are trapped behind). The rise time of this voltage pulse is a measure of the time it takes the carriers to separate. Because of the rapid diffusive conduction process on the electrodes, we can only see the fastest component of the rise time. And its temperature and voltage dependences strongly indicate that it is related to the electron tunneling.

A theoretical estimate of the electron tunneling time and its dependence on the electrical field can be obtained within the framework of coherent resonant tunneling

from the energy width  $\Delta E_{\text{HWHM}}$  of the resonance transmission peak, as  $\tau_T = \hbar/\Delta E_{\text{HWHM}}$ . We have done the calculation in the structure shown in Fig. 1(c), where only two periods of the quantum well structure are taken into account, because after tunneling through the second barrier, the electron is in the conduction band and can travel at the drift velocity corresponding to the applied field. The parameters used in the calculation were as follows: an electron mass of  $0.067m_0$  in GaAs and  $0.092m_0$  in AlGaAs ( $m_0$  is the free-electron mass), a conduction barrier height of 260 meV (corresponding to an offset ratio of 67:33), and a well thickness of 65 Å. The tunneling times  $\tau_T$  calculated for four different barrier thicknesses ranging from 50 to 62 Å are plotted versus field in Fig. 3(b). As expected, the calculated  $\tau_T$  is extremely sensitive to the barrier thickness: Between 50 and 62 Å,  $\tau_T$  increases 1 order of magnitude. Increased barrier thickness is also associated with smaller resonance fields. After a slight initial increase of  $\tau_T$  at low fields due to localization of the wave function in the asymmetric well, a steeply decreasing  $\tau_T$  is obtained, with a minimum corresponding to resonance of the  $2e$  level in the well on the right with the  $1e$  level in the well on the left [Fig. 1(c)]. The calculated curves in Fig. 3 are qualitatively similar to each other as well as to the experimental data; the calculation corresponding to a barrier thickness of 62 Å is probably the closest to the measured behavior. At the minimum, the calculated times are less than 1 ps, well below the time resolution in our experiment. However, the times we measure at the minimum and beyond it are well above our time resolution, and significantly larger than the calculated values. The difference cannot be accounted for by the estimated transit time of the electrons drifting through the structure ( $\sim 10$  ps). It is probably related to other processes that our simple calculation has neglected, such as elastic or inelastic scattering, or recapture by intersubband scattering. The intersubband scattering process which involves relaxation of the electron from the  $2e$  level in one well to the  $1e$  level in the second well is probably the most efficient. This process was recently reported to be very fast, within times of less than 3 ps in both the GaAs/AlGaAs (Ref. 17) and InGaAs/InAlAs (Ref. 18) systems.

In conclusion, our time-resolved electroabsorption measurements in GaAs/AlGaAs quantum wells clearly indicate that the main escape mechanism of the photoexcited electrons is tunneling. By studying the dependence of the sweep-out time on the applied field, we show how resonant tunneling enhances the electron escape rate. We calculate the field dependence of the electron tunneling times using the width of the transmission maxima in a resonant tunneling model. Although the qualitative behavior is remarkably well reproduced, this model gives

values in quantitative agreement with the experiment only off resonance. At resonance and beyond it, we measure times much longer than those calculated. A more rigorous description is needed, which should analyze the dynamics of the holes, as well as the scattering mechanisms of both carriers.

We thank F. Beltram and F. Capasso for illuminating discussions on resonant tunneling, and D. Oberli and J. Shah for sharing with us results of their most recent work on picosecond time-resolved luminescence in GaAs/AlGaAs quantum wells. The sample was expertly processed by D. J. Burrows.

<sup>(a)</sup>Present address: AT&T Bell Laboratories, Murray Hill, NJ 07974.

<sup>1</sup>B. Deveaud, J. Shah, T. C. Damen, B. Lambert, and A. Regreny, Phys. Rev. Lett. **58**, 2582 (1987).

<sup>2</sup>See the reviews by E. Esaki, IEEE J. Quantum Electron. **22**, 1611 (1986), and by F. Capasso, K. M. Mohammed, and A. Y. Cho, *ibid.* **22**, 1853 (1986).

<sup>3</sup>M. Tsuchiya, T. Matsusue, and H. Sakaki, Phys. Rev. Lett. **59**, 2356 (1987).

<sup>4</sup>S. Tarucha and K. Ploog, Phys. Rev. B **38**, 4198 (1988).

<sup>5</sup>H. Schneider, K. von Klitzing, and K. Ploog, Superlattices Microstruct. (to be published); H. Schneider and K. v. Klitzing, Phys. Rev. B **38**, 6160 (1989).

<sup>6</sup>Y. Horikoshi, A. Fischer, and K. Ploog, Phys. Rev. B **31**, 7859 (1985).

<sup>7</sup>M. K. Jackson, M. B. Johnson, D. H. Chow, T. C. McGill, and C. W. Nieh, Appl. Phys. Lett. **54**, 552 (1989).

<sup>8</sup>K. K. Choi, B. F. Levine, C. C. Bethea, J. Walker, and R. J. Malik, Phys. Rev. Lett. **59**, 2459 (1987).

<sup>9</sup>A. Larsson, P. A. Andrekson, S. T. Eng, and A. Yariv, IEEE J. Quantum Electron. **24**, 787 (1988).

<sup>10</sup>R. J. Manning, P. J. Bradley, A. Miller, J. S. Roberts, P. Mistry, and M. Pate, Electron. Lett. **24**, 854 (1988); Electron. Lett. (to be published).

<sup>11</sup>G. Livescu, D. A. B. Miller, T. Sizer, D. J. Burrows, J. E. Cunningham, A. C. Gossard, and J. H. English, Appl. Phys. Lett. **54**, 748 (1989).

<sup>12</sup>F. Capasso, K. Mohammed, and A. Y. Cho, Appl. Phys. Lett. **48**, 478 (1986).

<sup>13</sup>R. Sauer, K. Thonke, and W. T. Tsang, Phys. Rev. Lett. **61**, 609 (1988).

<sup>14</sup>D. A. B. Miller, Opt. Eng. **26**, 368 (1987); G. Livescu and D. A. B. Miller, Proc. Int. Soc. Opt. Eng. **825**, 69 (1988).

<sup>15</sup>D. A. B. Miller, D. S. Chemla, T. C. Damen, A. C. Gossard, W. Wiegmann, T. H. Wood, and C. A. Burrus, Phys. Rev. B **32**, 1043 (1985).

<sup>16</sup>We are indebted to T. Harris and M. Lamont for photoluminescence measurements, and to G. Chu for transmission electron microscopy measurements.

<sup>17</sup>A. Seilmeier, Superlattices Microstruct. (to be published).

<sup>18</sup>R. J. Bauerle, T. Elsasser, W. Kaiser, H. Lobentzner, W. Stolz, and K. Ploog, Phys. Rev. B **38**, 4307 (1988).